



Cloud condensation nucleus activity of secondary organic aerosol particles mixed with sulfate

Stephanie M. King,¹ Thomas Rosenoern,¹ John E. Shilling,¹ Qi Chen,¹ and Scot T. Martin¹

Received 16 April 2007; revised 30 July 2007; accepted 15 October 2007; published 21 December 2007.

[1] The cloud condensation nucleus (CCN) activity of organic-sulfate particles was investigated using a steady-state environmental chamber. The organic component consisted of secondary organic aerosol (SOA) generated in the dark from 24 ± 2 ppb α -pinene for conditions of 300 ± 5 ppb ozone, $40 \pm 2\%$ relative humidity, and $25 \pm 1^\circ\text{C}$, with the organic mass loading in the chamber ranging from 23 to $37 \mu\text{g m}^{-3}$. CCN analysis was performed for 80- to 150-nm particles having variable organic-sulfate volume fractions, which were estimated from the diameter of the organic-sulfate particle relative to that of the seed as well as independently from mass spectra. Critical supersaturation, which increased for greater SOA volume fraction and smaller particle diameter, was well predicted by a Köhler model having two components, one for ammonium sulfate and another for SOA. The entire data set could be successfully modeled by a single suite of effective chemical parameters for SOA. The results suggest that the effects of limited organic solubility in mixed SOA-sulfate particles may be reliably omitted in the treatment of cloud droplet formation. **Citation:** King, S. M., T. Rosenoern, J. E. Shilling, Q. Chen, and S. T. Martin (2007), Cloud condensation nucleus activity of secondary organic aerosol particles mixed with sulfate, *Geophys. Res. Lett.*, *34*, L24806, doi:10.1029/2007GL030390.

1. Introduction

[2] Tropospheric aerosol particles affect the earth's climate by several mechanisms, including among others their potential to form cloud droplets. Current understanding of the activation potential of cloud condensation nuclei (CCN) remains incomplete, especially for organic compounds, which constitute a large mass fraction of ambient fine particulate matter [Fuzzi *et al.*, 2006]. Particulate organic matter originates from both primary and secondary sources, the latter of which include the oxidation of anthropogenic and biogenic emissions. Biogenic emissions, including isoprene, monoterpenes, and sesquiterpenes, are the larger source of global secondary organic aerosol (SOA) [Kanakidou *et al.*, 2005].

[3] In atmospheric particles, organic compounds are often internally mixed with inorganic species, especially sulfates [Murphy *et al.*, 2006]. Given that the consideration of the inorganic fraction alone does not sufficiently explain CCN activation [Novakov and Penner, 1993; Facchini *et al.*, 1999], several laboratory studies have investigated the CCN activity of internally mixed particles having both

inorganic and organic species [Cruz and Pandis, 1998; Raymond and Pandis, 2003; Shantz *et al.*, 2003; Bilde and Svenningsson, 2004; Broekhuizen *et al.*, 2004; Lohmann *et al.*, 2004; Henning *et al.*, 2005]. Recent laboratory CCN results of mixed particles have also been used in model analyses to infer thermodynamic properties of the organic component [Padró *et al.*, 2007]. The organic fraction in these studies consisted of at most a few organic species, whereas atmospheric SOA contains thousands. To bridge this gap, the CCN properties of SOA have been investigated using environmental chambers, with the focus thus far on particles of purely organic compositions [Hartz *et al.*, 2005; VanReken *et al.*, 2005; Prenni *et al.*, 2007]. Given the widespread atmospheric occurrence of mixed SOA-sulfate particles and the absence of previous laboratory investigations of the CCN activity of this particle class, the study described in this paper was initiated.

2. Experiment

[4] An environmental chamber, consisting of a constant temperature room housing a flexible Teflon bag (Welch Fluorocarbon Inc.) of approximately 5 m^3 , was operated continuously for several weeks in a feedback-controlled constant-volume mode, for which the flow in equaled the flow out. A schematic diagram of the experimental setup is shown in Figure S1.¹ The conditions that were monitored and held constant were temperature ($25 \pm 1^\circ\text{C}$), relative humidity (RH) ($40 \pm 2\%$), and ozone concentration (300 ± 5 ppb). The NO_x concentration remained below 1 ppb. For the approximation of a completely mixed flow reactor, the corresponding residence time in the chamber was 4 hours. Steady-state conditions of all measurables were reached after 24 hours and maintained indefinitely.

[5] Dry $(\text{NH}_4)_2\text{SO}_4$ seed particles and α -pinene (Aldrich, 98%) vapor were continuously introduced into the bag. Sulfate particles from a TSI 3076 atomizer were passed through a 160-cm silica gel diffusion dryer (RH < 10%), followed by a ^{85}Kr bipolar charger and a differential mobility analyzer (DMA₁, TSI 3071). DMA₁ was operated with sheath and monodisperse aerosol flows of 10 and 2 Lpm, respectively, to obtain a quasi-monodisperse seed aerosol. A syringe pump injected a 1:600 (v/v) mixture of α -pinene and 1-butanol (serving as an OH scavenger) into a bulb that was flushed with clean air. Based on the flow rates, the α -pinene available for reaction in the bag had an equivalent mixing ratio of 24 ± 2 ppb. Reaction of α -pinene by dark ozonolysis led to the formation of SOA, which condensed onto the seed particles and induced particle diameter growth. The SOA mass loading varied between 23 and

¹School of Engineering and Applied Sciences, Harvard University, Cambridge, Massachusetts, USA.

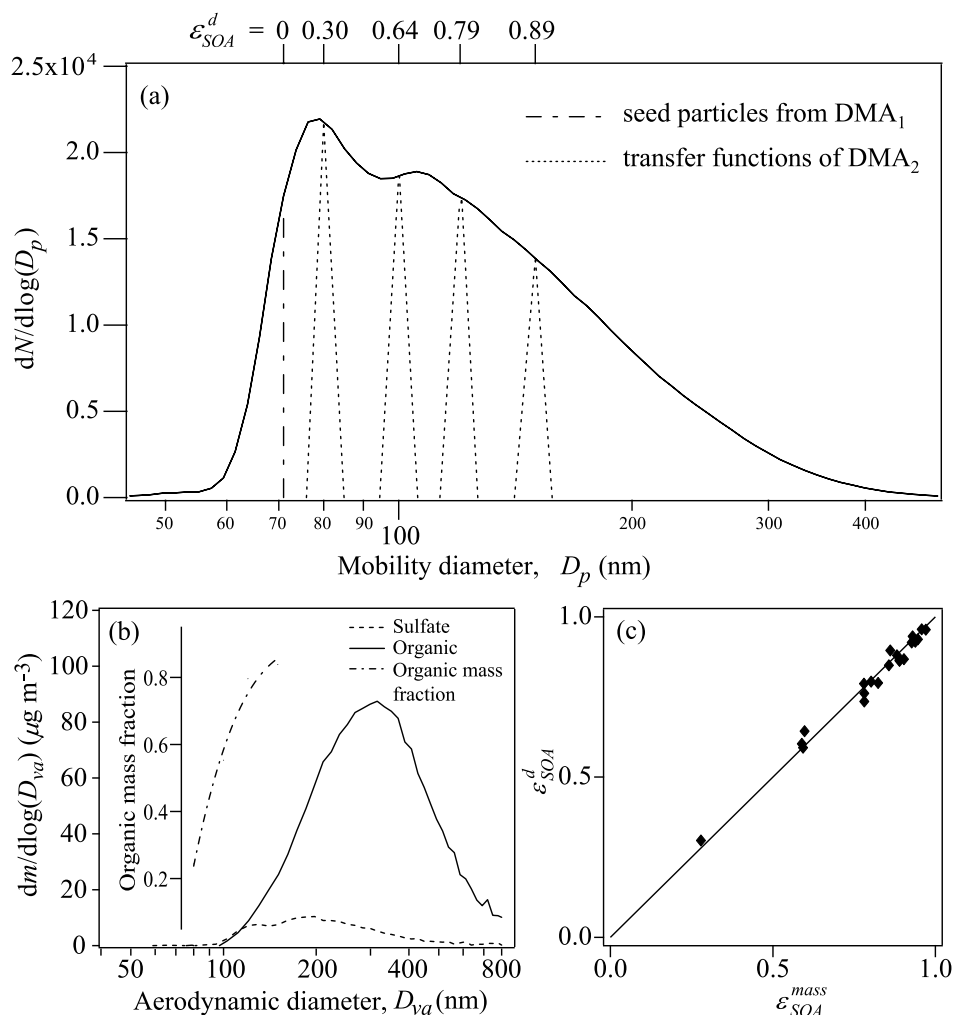


Figure 1. Organic volume fraction (ϵ_{SOA}) of SOA mixed with sulfate. (a) Representative number-weighted size distribution of particles exiting the environmental chamber for a seed diameter of 71 nm. The corresponding diameter-based organic volume fractions (ϵ_{SOA}^d) are shown along the upper axis. (b) Representative mass-weighted size distribution of particles exiting the environmental chamber for a seed diameter of 71 nm as measured by the HR-ToF-AMS. The calculated organic mass fraction is also shown. (c) Comparison of organic volume fraction (ϵ_{SOA}^d) calculated from seed and final particle diameters to the volume fraction (ϵ_{SOA}^{mass}) calculated from AMS mass measurements. Data for seed particles of 27 and 31 nm are omitted in Figure 1c because sulfate loadings were below the detection limit of the AMS. Comparison to the shown 1:1 line yields an r-squared value of 0.98.

$37 \mu\text{g m}^{-3}$ during the course of the experiments. The possibility of externally mixed organic particles was ruled out because no nucleation events were observed and because measured particles were larger than the seed particles.

[6] The aerosol in the outflow from the chamber passed through a diffusion tube having an outer annulus filled with ozone destruction catalyst. The flow was then split for simultaneous sampling by (1) a scanning mobility particle sizer (SMPS, TSI 3936), (2) a condensation particle counter (CPC₁, TSI 3022), (3) an Aerodyne high-resolution time-of-flight aerosol mass spectrometer (HR-ToF-AMS) [DeCarlo *et al.*, 2006], and (4) a DMA₂ (TSI 3081, sheath:sample flow ratio of 10:1), the outflow of which was split to a CPC₂ (TSI 3772) and a cloud condensation nucleus counter (CCNC, DMT Inc.) [Roberts and Nenes, 2005]. Particles were recharged before sampling by the SMPS and DMA₂. Calibration of the CCNC was performed with $(\text{NH}_4)_2\text{SO}_4$ at supersaturations of 0.090%, 0.26%, 0.43%, 0.60%, and

1.02% using equations described by Shilling *et al.* [2007] (Table S1). Rose *et al.* [2007] discuss in further detail the calibration and measurement uncertainties of the DMT CCNC. DMA₂ was used to select a monodisperse aerosol from the chamber, and the activated CCN fraction (F_a) was calculated as the number concentration of activated droplets counted by the CCNC divided by the total number concentration detected by CPC₂. In the experimental procedure, F_a was measured for increasing supersaturation, and the data were fit with a sigmoidal curve using a filter to omit the effect of multiply charged particles [Asa-Awuku *et al.*, 2007]. The supersaturation at which $F_a = 0.5$ was defined as the critical supersaturation (S_c).

3. Multiple-Component Köhler Model

[7] The model used to describe the CCN activity of internally mixed organic-sulfate particles is based on Köhler

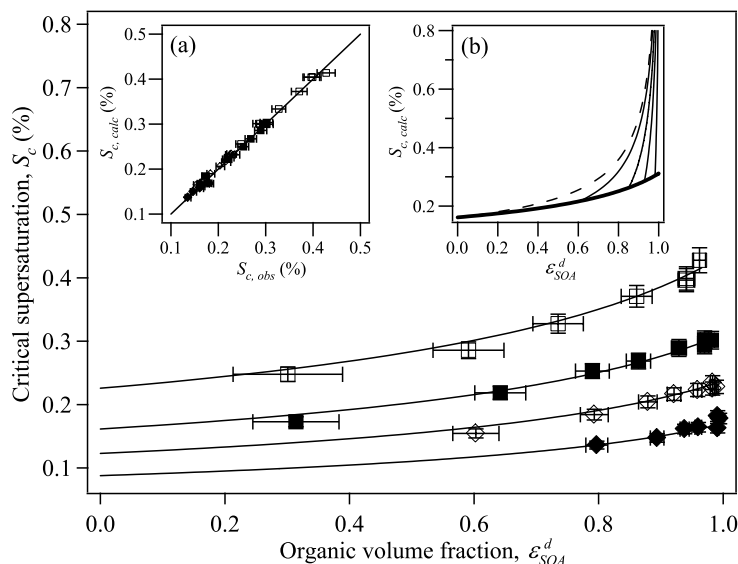


Figure 2. Critical supersaturation (S_c) for 50% CCN activation of SOA particles internally mixed with sulfate. Data are shown for four particle mobility diameters (open square, 80 nm; solid square, 100 nm; open diamond, 120 nm; and solid diamond, 150 nm) for increasing organic volume fraction (ε_{SOA}^d). Curves represent modeled values (equations (1) to (3)) using a single set of parameters (see Table 1). Curves for each diameter are drawn from $\varepsilon_{SOA}^d = 0$ to the largest measured ε_{SOA}^d . Error bars in ε_{SOA}^d are 95% confidence intervals based on the geometric standard deviations of the mobility size distributions of the seed particles and the mixed particles. Error bars for S_c values represent 95% confidence intervals based on four reproducibility experiments performed over 30 days for a seed diameter of 31 nm. The data shown are tabulated in Table S2, and representative CCN activation curves of SOA particles having ammonium sulfate cores of 51-nm mode diameter are shown in Figure S4. (a) Comparison of modeled S_c to observed S_c for all particle diameters. Comparison to the shown 1:1 line yields an r-squared value of 0.99. (b) Modeled S_c values of 100-nm mixed SOA-sulfate particles for a limited-solubility system with varying values of $C_{sat,SOA}$. The thick solid curve represents a fully soluble case, and the dashed curve represents a fully insoluble case. The four remaining curves correspond to limited-solubility particles having $C_{sat,SOA}$ values of 0.004, 0.015, 0.030, and 0.070 $\text{g g}^{-1} \cdot \text{H}_2\text{O}$.

[1936] theory, which expresses the vapor pressure of water over an aqueous droplet as follows:

$$s = a_w \exp\left(\frac{4\sigma M_w}{RT\rho_w D_{aq}}\right), \quad (1)$$

where s is the saturation ratio relative to a flat surface of liquid water, a_w is the water activity of the solution, σ is the solution-vapor surface tension, M_w is the molecular weight of pure water, R is the universal gas constant, T is the solution temperature, ρ_w is the density of pure water, and D_{aq} is the aqueous particle diameter. The maximum of equation (1) (s_{max}) corresponds to the critical supersaturation $S_c = s_{\text{max}} - 1$.

[8] The water activity for a multi-component solution is given by:

$$a_w = \frac{n_w}{n_w + \sum_k i_k n_k}, \quad (2)$$

where n_w is the number of moles of water, n_k is the number of moles of species k in solution, and i_k is the corresponding van't Hoff factor. The possibility of limited solubility of species k is incorporated by using an expression adapted from Henning *et al.* [2005]:

$$n_k = \min\left[\frac{(D_{aq}^3 - D_0^3)\rho'_w C_{sat,k}}{M_k}, \frac{\varepsilon_k D_0^3 \rho_k}{M_k}\right] \frac{\pi}{6}, \quad (3)$$

where $C_{sat,k}$ is the saturation concentration of species k ($\text{g g}^{-1} \cdot \text{H}_2\text{O}$), ρ'_w is the density of water in solution (taken equal to ρ_w for dilute conditions), ε_k is the volume fraction in the dry particle, ρ_k is the density, D_0 is the diameter of the dry particle, and M_k is the molecular weight.

4. Results and Discussion

[9] CCN activity was investigated for particles having midpoint mobility diameters of 80, 100, 120, and 150 nm, each varying in organic volume fraction depending on sulfate seed diameter (27, 31, 41, 51, 59, 71, or 88 nm). Figure 1a shows a typical number size distribution of particles exiting the chamber for a seed diameter of 71 nm. The organic volume fraction (ε_{SOA}^d) was calculated from the increase in particle diameter relative to the seed particle. Spherical dry particles were assumed. In addition, the size-dependent sulfate and organic mass loadings were measured with the HR-ToF-AMS, from which the organic mass fraction was calculated and converted using organic density to a second, independent measurement of volume fraction ($\varepsilon_{SOA}^{\text{mass}}$) (Figure 1b). The organic density ($\rho_{SOA} = 1.4 \pm 0.1 \text{ g cm}^{-3}$) was determined from the mode diameters of the vacuum-aerodynamic size distribution and the mobility size distribution, assuming a spherical particle shape and including a correction for the density of ammonium sulfate [DeCarlo *et al.*, 2004; Katrib *et al.*, 2005]. A scatter plot of ε_{SOA}^d and $\varepsilon_{SOA}^{\text{mass}}$ shows good agreement (Figure 1c). AMS measure-

Table 1. Parameters Used in Köhler Model to Calculate S_c^a

Parameter	Value
Surface tension, σ	0.0725 N m ⁻¹
Density of (NH ₄) ₂ SO ₄ , ρ_{AS}	1.77 g cm ⁻³
van't Hoff factor of (NH ₄) ₂ SO ₄ , i_{AS}	2.2
Molecular weight of (NH ₄) ₂ SO ₄ , M_{AS}	132.14 g mol ⁻¹
Effective SOA density, ρ_{SOA}	1.4 g cm ⁻³
Effective SOA van't Hoff factor, i_{SOA}	1
Effective SOA molecular weight, M_{SOA}	178 g mol ⁻¹
Saturation concentration of SOA, $C_{sat,SOA}$	0.070 g g ⁻¹ H ₂ O ^b

^aSee equations (1) to (3).

^bLower limit (see text).

ments also confirmed that the SOA chemistry was stable during the course of experiments (Figure S3). A full V-mode ToF-AMS spectrum of SOA having a 71-nm ammonium sulfate core is also shown in Figure S2. For example, the ratio of the signal intensity at m/z 43 to that at m/z 44 fell between 1.24 and 1.41 for all experiments.

[10] Critical supersaturation (S_c) increased for greater SOA volume fraction and smaller particle diameter (Figure 2 and Table S2). The curves in Figure 2 show the least-squares fit of a two-component model that uses equations (1) to (3). The model consists of ammonium sulfate as one chemical component and SOA as a second effective chemical component (i.e., SOA is a mixture consisting of many organic species). The effective SOA molecular weight (M_{SOA}) was obtained as an optimized model fit to the entire data set shown in Figure 2 for fixed values of the surface tension (σ), the effective SOA density (ρ_{SOA}), and the effective van't Hoff factor of SOA (i_{SOA}) (Table 1). The optimization had no sensitivity to the effective saturation concentration of the organic component ($C_{sat,SOA}$) provided that a lower limit of 0.070 g g⁻¹·H₂O was exceeded. The values of i_{SOA} and σ were assumed equal to 1 and 0.0725 N m⁻¹, respectively. M_{SOA} , the target of the global optimization, was constrained as 178 ± 3 g mol⁻¹ based on the least-squares fit of the entire data set using a Monte Carlo approach to vary S_c values within their uncertainties.

[11] The sensitivity of the modeled S_c was evaluated by applying perturbations of approximately 10% to each input parameter (σ , ρ_{SOA} , i_{SOA} , and M_{SOA}). For the range of perturbations investigated, Table S3 shows that changes in σ have the greatest effect on the modeled S_c . Correspondingly, the constrained value of M_{SOA} depends most strongly on the assumed value of σ . Further sensitivity studies were therefore performed by simultaneously optimizing for both σ and M_{SOA} , obtaining values of 0.0702 N m⁻¹ and 202 g mol⁻¹, respectively. This value of σ , which is close to that of pure water, suggests the absence of significant surface-tension lowering by organic molecules. For values of σ between 0.0702 and 0.0725 N m⁻¹, M_{SOA} ranges from 178 to 202 g mol⁻¹.

[12] An implication of $C_{sat,SOA} > 0.070$ g g⁻¹·H₂O is that the mixed organic-sulfate particles were fully solvated at activation, up to the largest measured organic fraction. The raw data further support this model-based conclusion, notably through the absence of an abrupt discontinuity in S_c for increasing ε_{SOA}^d in Figure 2, contrary to the behavior of a limited-solubility system (inset b) [Henning et al., 2005]. Moreover, adjustments in the values of the SOA parameters in Table 1 do not allow the data of Figure 2 to be

fit by a limited-solubility assumption (analysis not shown). As indicated in inset b, the ε_{SOA}^d at which the discontinuity occurs depends on $C_{sat,SOA}$. Thus, the lower limit of $C_{sat,SOA}$ for this study can be calculated from the largest measured ε_{SOA}^d for which there is no discontinuity. This lower limit is, however, much higher than expected given the chemical composition of dark ozonolysis α -pinene SOA [Glasius et al., 2000]. To explain the greater apparent organic solubility, we hypothesize that the high effective SOA solubility arises because the particles are either supersaturated aqueous solutions of organic material at 40% RH [Bilde and Svenningsson, 2004] or liquids or amorphous solids even at low water activity [Marcolli et al., 2004].

[13] Using the effective SOA parameters, we can predict the CCN activity of pure SOA particles and thereby compare with previous CCN studies that were performed in the absence of inorganic seed particles. CCN data from three studies of the dark ozonolysis of α -pinene SOA are shown in Figure 3 [Hartz et al., 2005; VanReken et al., 2005; Prenni et al., 2007]. The solid line corresponds to the effective SOA parameters of this study, thus implicitly assuming no solubility-limited behavior for $\varepsilon_{SOA}^d \rightarrow 1$. The dotted line is calculated using the parameters of Hartz et al. [2005]. Both model results agree with the data of Prenni et al. [2007] and with each other, which is expected because the M_{SOA} : ρ_{SOA} ratio of 146 cm³ mol⁻¹ from Hartz et al. is similar to that of 127 ± 12 cm³ mol⁻¹ determined in this study (see equation (3)). The ρ_{SOA} value of 1.2 g cm⁻³ assumed by Hartz et al. is lower than our measured ρ_{SOA} value of 1.4 ± 0.1 g cm⁻³. The M_{SOA} value of 178 to 202 g mol⁻¹ of this study is slightly greater than the value of 175 g mol⁻¹ of Hartz et al., who estimated M_{SOA} using literature-based reports of α -pinene SOA products. Possible hypotheses to explain the different values of M_{SOA} include (1) that the product species reported in the literature omit high molecular weight oligomers or (2) that SOA composition and hence M_{SOA} are not fixed quantities, possibly depending on reaction conditions and mass loadings. The results for M_{SOA} can also differ depending on the theoretical

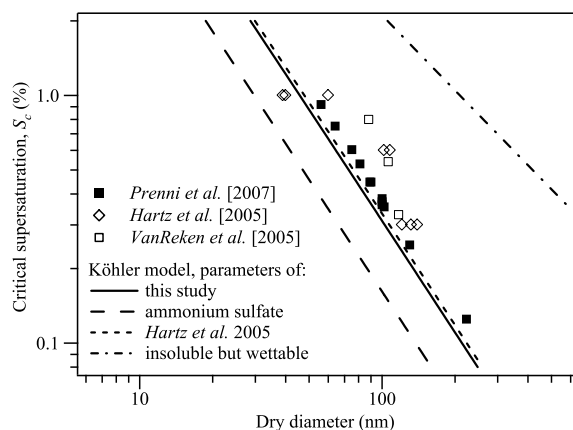


Figure 3. Observed critical supersaturations for increasing dry particle diameter from Hartz et al. [2005], VanReken et al. [2005], and Prenni et al. [2007] for α -pinene SOA from dark ozonolysis (no inorganic component). Experimental data are compared to models using parameters from this study (Table 1) and from Hartz et al. [2005].

framework used for analysis of CCN observations, most notably in the treatment of water activity. For example, the model described in this study assumes the additivity of species (see equation (2)) because of the absence of knowledge on the interaction terms between SOA molecules and ammonium sulfate ions. Therefore, M_{SOA} should be regarded as an effective molecular weight and not a physical molecular weight.

5. Conclusions and Atmospheric Implications

[14] The results of this study show that the CCN behavior of mixed multi-component organic-sulfate particles is well predicted by a two-component Köhler model. The critical supersaturations for a range of atmospherically relevant sizes and compositions lie between 0.1% and 0.5%, well within the range of possible atmospheric conditions. Findings from this and other related laboratory studies of CCN activity serve as the physical basis to describe aerosol-cloud interactions in general circulation models as well as in explicit cloud-resolving models. Many treatments have supposed the necessity of employing a modified Köhler theory that incorporates the effects of limited solubility [Nenes and Seinfeld, 2003]. Our study implies that computations of CCN spectra can be simplified (yet remain accurate) by omitting the consideration of limited solubility for the mixed organic-sulfate particles prevalent in the atmosphere, at least for the range of conditions and types of particles considered in this study.

[15] **Acknowledgments.** This material is based upon work supported by the National Science Foundation under Grant ATM-0513463. SMK acknowledges support from the EPA STAR fellowship program. TR acknowledges support from the Danish Agency for Science Technology and Innovation under Grant 272-06-0318. We thank the Carnegie Mellon University Air Quality Laboratory for helpful consultation.

References

- Asa-Awuku, A., A. Nenes, A. P. Sullivan, C. J. Hennigan, and R. J. Weber (2007), Investigation of molar volume and surfactant characteristics of water-soluble organic compounds in biomass burning aerosol, *Atmos. Chem. Phys. Discuss.*, *7*, 3589–3627.
- Bilde, M., and B. Svenningsson (2004), CCN activation of slightly soluble organics: The importance of small amounts of inorganic salt and particle phase, *Tellus*, *56*, 128–134.
- Broekhuizen, K., P. P. Kumar, and J. P. D. Abbatt (2004), Partially soluble organics as cloud condensation nuclei: Role of trace soluble and surface active species, *Geophys. Res. Lett.*, *31*, L01107, doi:10.1029/2003GL018203.
- Cruz, C. N., and S. N. Pandis (1998), The effect of organic coatings on the cloud condensation nuclei activation of inorganic atmospheric aerosol, *J. Geophys. Res.*, *103*, 13,111–13,123.
- DeCarlo, P. F., J. G. Slowik, D. R. Worsnop, P. Davidovits, and J. L. Jimenez (2004), Particle morphology and density characterization by combined mobility and aerodynamic diameter measurements. Part 1: Theory, *Aerosol Sci. Technol.*, *38*, 1185–1205.
- DeCarlo, P. F., et al. (2006), Field-deployable, high-resolution, time-of-flight aerosol mass spectrometer, *Anal. Chem.*, *78*, 8281–8289.
- Facchini, M. C., M. Mircea, S. Fuzzi, and R. J. Charlson (1999), Cloud albedo enhancement by surface-active organic solutes in growing droplets, *Nature*, *401*, 257–259.
- Fuzzi, S., et al. (2006), Critical assessment of the current state of scientific knowledge, terminology, and research needs concerning the role of organic aerosols in the atmosphere, climate, and global change, *Atmos. Chem. Phys.*, *6*, 2017–2038.
- Gladius, M., M. Lahaniati, A. Calogirou, D. Di Bella, N. R. Jensen, J. Hjorth, D. Kotzias, and B. R. Larsen (2000), Carboxylic acids in secondary aerosols from oxidation of cyclic monoterpenes by ozone, *Environ. Sci. Technol.*, *34*, 1001–1010.
- Hartz, K. E. H., T. Rosenorn, S. R. Ferchak, T. M. Raymond, M. Bilde, N. M. Donahue, and S. N. Pandis (2005), Cloud condensation nuclei activation of monoterpene and sesquiterpene secondary organic aerosol, *J. Geophys. Res.*, *110*, D14208, doi:10.1029/2004JD005754.
- Henning, S., T. Rosenorn, B. D'Anna, A. A. Gola, B. Svenningsson, and M. Bilde (2005), Cloud droplet activation and surface tension of mixtures of slightly soluble organics and inorganic salt, *Atmos. Chem. Phys.*, *5*, 575–582.
- Kanakidou, M., et al. (2005), Organic aerosol and global climate modelling: A review, *Atmos. Chem. Phys.*, *5*, 1053–1123.
- Katrib, Y., S. T. Martin, Y. Rudich, P. Davidovits, J. T. Jayne, and D. R. Worsnop (2005), Density changes of aerosol particles as a result of chemical reaction, *Atmos. Chem. Phys.*, *5*, 275–291.
- Köhler, H. (1936), The nucleus in and the growth of hygroscopic droplets, *Trans. Faraday Soc.*, *32*, 1152–1161.
- Lohmann, U., K. Broekhuizen, R. Leaitch, N. Shantz, and J. Abbatt (2004), How efficient is cloud droplet formation of organic aerosols?, *Geophys. Res. Lett.*, *31*, L05108, doi:10.1029/2003GL018999.
- Marcollì, C., B. P. Luo, and T. Peter (2004), Mixing of the organic aerosol fractions: Liquids as the thermodynamically stable phases, *J. Phys. Chem. A*, *108*, 2216–2224.
- Murphy, D. M., D. J. Cziczo, K. D. Froyd, P. K. Hudson, B. M. Matthew, A. M. Middlebrook, R. E. Peltier, A. Sullivan, D. S. Thomson, and R. J. Weber (2006), Single-particle mass spectrometry of tropospheric aerosol particles, *J. Geophys. Res.*, *111*, D23S32, doi:10.1029/2006JD007340.
- Nenes, A., and J. H. Seinfeld (2003), Parameterization of cloud droplet formation in global climate models, *J. Geophys. Res.*, *108*(D14), 4415, doi:10.1029/2002JD002911.
- Novakov, T., and J. E. Penner (1993), Large contribution of organic aerosols to cloud-condensation-nuclei concentrations, *Nature*, *365*, 823–826.
- Padró, L. T., A. Asa-Awuku, R. Morrison, and A. Nenes (2007), Inferring thermodynamic properties from CCN activation experiments: single-component and binary aerosols, *Atmos. Chem. Phys.*, *7*, 5263–5274.
- Prenti, A. J., M. D. Petters, S. M. Kreidenweis, and P. J. DeMott (2007), Cloud droplet activation of secondary organic aerosol, *J. Geophys. Res.*, *112*, D10223, doi:10.1029/2006JD007963.
- Raymond, T. M., and S. N. Pandis (2003), Formation of cloud droplets by multicomponent organic particles, *J. Geophys. Res.*, *108*(D15), 4469, doi:10.1029/2003JD003503.
- Roberts, G. C., and A. Nenes (2005), A continuous-flow streamwise thermal-gradient CCN chamber for atmospheric measurements, *Aerosol Sci. Technol.*, *39*, 206–221.
- Rose, D., G. P. Frank, U. Dusek, S. S. Gunthe, M. O. Andreae, and U. Poschl (2007), Calibration and measurement uncertainties of a continuous-flow cloud condensation nucleus counter (DMT-CCNC): CCN activation of ammonium sulfate and sodium chloride aerosol particles in theory and experiment, *Atmos. Chem. Phys. Discuss.*, *7*, 8193–8260.
- Shantz, N. C., W. R. Leaitch, and P. F. Caffrey (2003), Effect of organics of low solubility on the growth rate of cloud droplets, *J. Geophys. Res.*, *108*(D5), 4168, doi:10.1029/2002JD002540.
- Shilling, J. E., S. M. King, M. Mochida, D. R. Worsnop, and S. T. Martin (2007), Mass spectral evidence that small changes in composition caused by oxidative aging processes alter aerosol CCN properties, *J. Phys. Chem. A*, *111*, 3358–3368.
- VanReken, T. M., N. L. Ng, R. C. Flagan, and J. H. Seinfeld (2005), Cloud condensation nucleus activation properties of biogenic secondary organic aerosol, *J. Geophys. Res.*, *110*, D07206, doi:10.1029/2004JD005465.

Q. Chen, S. M. King, S. T. Martin, T. Rosenorn, and J. E. Shilling, School of Engineering and Applied Sciences, Harvard University, Cambridge, MA 02138, USA. (scot_martin@harvard.edu)